Perspective of the Uniaxial Wavelet-transformed FDTD Scheme

Winfried Bilgic [1], Ingo Wolff [2], and Daniel Erni [1]

[1] Faculty of Electrical Engineering, General and Theoretical Electrical Engineering (ATE)
University of Duisburg Essen, Bismarckstr. 81, D-47048 Duisburg, Germany
wbilgic@ieee.org, daniel.erni@uni-due.de

[2] IMST GmbH
Carl-Friederich-Gauss Str.2, D-47475 Kamp-Lintfort, Germany
wolff@imst.de

Abstract: In this paper an investigation on computational efficiency for a spatial wavelet-transformed FDTD scheme is presented. The spatial transformation process has many degrees of freedom, like the wavelet filter, which direction of transformation and his corresponding scale. Their influence on the resulting picture of the time-depended electromagnetic field is important in finding the right settings. Whereas only a right chosen neglecting strategy of wavelet coefficients makes the scheme computational efficient and should not have negative impact on integral parameters. It turned out that an uniaxial transformation scheme on planar microwave structures in the direction of substrate height is the best choice in terms of pre-processing time and computation error. In combination with two introduced neglecting strategies onto the wavelet coefficients the influence on scattering parameter is small enough to be omitted and the appropriate computational effort is less in comparison with classical FDTD schemes.

Keywords: WT-FDTD, MRSD, uniaxial wavelet-transformed, spatial wavelet-transformed, multi-resolution, static grid, dynamic grid, adaptive grid.

1. Introduction

Future problems will always need an increasing demand for numerical capacity. As the working horse in computational electrodynamics the FDTD method has been successfully extended over the years with absorbing boundaries, different excitation modes, anisotropic, dispersive and nonlinear material, near to far-field transformation, the incorporation of thermal conduction, but the progress of the method with always be limited by computational resources. The improvement of the "leap-frog" algorithm was topic on two branches of the classical FDTD scheme. Both branches use the compression ability of the discrete wavelet transformation. The first branch by Krumpholz and Katehi [1] applied the transformation scheme in time domain called multi-resolution time-domain (MRTD) method, whereas the second branch by Werthen and Wolff [2, 3] uses the discrete wavelet transformation in the spatial domain called wavelet-transformed FDTD or multi-resolution spatial-domain (WT-FDTD or MRSD). The designated scheme set up the spatial operators of the FDTD scheme as usual and applied afterwards a discrete wavelet transformation. The transformation process translates the spatial operators into the wavelet-domain to use the multi-resolution capabilities, but those operators also boost their access on wavelet coefficients to all resolution grids. The transformed "leap-frog" cycle yields into more numerical effort, which is depended on the chosen wavelet filter, scale of transformation and on directions that are included in the transformation process. Decrease of the numerical effort is possible by setting unnecessary wavelet coefficients to zero without losing important field information. This paper gives a short introduction

into the spatial wavelet-transformed FDTD and two strategies to determine unnecessary wavelet coefficients. In the second part we extend the influence of those strategies on scattering parameter and their resulting numerical efficiency for one-dimensional FDTD calculations, partly presented in [4]. Based on comprehensive empirical investigations on two microwave structures we determine which wavelet filter and how many directions of transformation have the best properties for the wavelet-transformed FDTD scheme. We conclude our outline with a short summary in section 5.

2. Spatial wavelet-transformed FDTD

The first integral part of the WT-FDTD scheme consists of the transformation of the derivative and material operators in space to achieve multi-resolution characteristic. Using a graded FDTD mesh in the original domain allows a higher spatial resolution when sampling specific regions such as metallic edges or material transition, with higher density by obtaining better numerical efficiency, but the result of higher sampling yields to over sampled location especially near the edges of the computational windows (Fig.1a).

a) b)

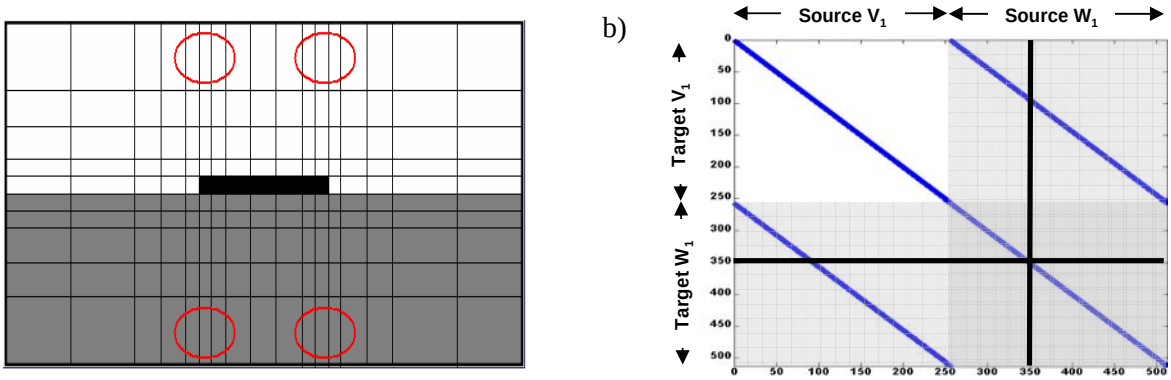

Fig.1 a) A typical graded mesh discretization for a microstrip-line with over-sampled regions.
b) An interlinked material and derivative operator in wavelet domain in matrix view, the negligence of target and source point via operator (horizontal and vertical line) makes the operator representation efficient.

The multi-resolution grid of the WT-FDTD scheme could consider those over sampled regions by neglecting their assign wavelet-coefficients. For a simpler and more compact notation for the WT-FDTD update equations, components and direction indices are numbered in a modulo-three sense, e.g. $E_x = E_D$, $E_y = E_{D+1}$ and $E_z = E_{D-1}$. Starting with the classical FDTD update equations (Ampere's law) and applying only a wavelet-transformation in *z*-direction, we yield

$$
\begin{aligned}
E_D^{n+1} &= E_D^n + \frac{\Delta t}{\varepsilon_{r,D}}\left[\partial_{D+1} H_{D-1}^{n+\frac{1}{2}} - \partial_{D-1} H_{D+1}^{n+\frac{1}{2}}\right] \\
WT_z \otimes E_D^{n+1} &= WT_z \otimes \left[E_D^n + \frac{\Delta t}{\varepsilon_{r,D}}\left(\partial_{D+1} H_{D-1}^{n+\frac{1}{2}} - \partial_{D-1} H_{D+1}^{n+\frac{1}{2}}\right)\right] \\
\tilde{E}_D^{n+1} &= \tilde{E}_D^n + WT_z \otimes \left[M_D\left(\partial_{D+1} H_{D-1}^{n+\frac{1}{2}} - \partial_{D-1} H_{D+1}^{n+\frac{1}{2}}\right)\right] \\
\tilde{E}_D^{n+1} &= \tilde{E}_D^n + WT_z \otimes M_D \otimes WT_z^{-1}\left[\partial_{D+1} WT_z \otimes H_{D-1}^{n+\frac{1}{2}} - WT_z \otimes \partial_{D-1} \otimes WT_z^{-1} \otimes WT_z \otimes H_{D+1}^{n+\frac{1}{2}}\right] \\
\tilde{E}_D^{n+1} &= \tilde{E}_D^n + \tilde{M}_D\left[\partial_{D+1} \tilde{H}_{D-1}^{n+\frac{1}{2}} - \tilde{\partial}_{D-1} \tilde{H}_{D+1}^{n+\frac{1}{2}}\right] \qquad \text{with} \quad WT_z \otimes WT_z^{-1} = I
\end{aligned}
\tag{1}
$$

The Faraday equation can be transformed in the same sense. Since we apply a linear transformation we inherit all advantages of the classical FDTD scheme, this includes the well-known stability condition. It's worth mentioning, that the material operator comprised all three dimensions, whereas the derivative operator is a 1D operator and only effective to its assigned direction. Our one-dimensional transformation in *z*-direction causes the untransformed derivative operator $\partial_{D+1}(\partial_y, \partial_x)$, which assigned direction does not agree to the transformation direction. After the discrete wavelet transformation the field-components are spatially divided into an averaging field V_1 and a detail field W_1. The correlation of those segments V_1 and W_1 is reconstituted by the transformed material operator $\tilde{M}_D$ and the derivative operator $\tilde{\partial}_{D-1}$. Their accessing structure simultaneously uses both segments (Fig.1b). The thoughtless use of the transformed operators yields into longer numerical computation. This problem is tackled in the second integral part of the WT-FDTD scheme, which neglects unnecessary wavelet coefficients by setting the specific operator coefficients to zero (Fig.1b). The detail field W_1 is the main region for neglecting wavelet coefficients, since the electromagnetic field is mostly smooth and continuous and the resulting differences are small enough to be omitted. Taking the whole scheme in comparison with approved wavelet applications like JPEG 2000 [8], the scheme applies the multi-resolution grid, compression and self-similarity characteristics on operators instead of any formatted picture data. Whereas the JPEG 2000 research were focused on finding the most appropriate wavelet filter and examine the resulting picture based on different compression techniques, our application needs as well the knowledge which appropriate wavelet filter has the lowest numerical effort by having good results for integral parameters, e.g. scattering parameter or far-field pattern.

3. Scattering parameter and numerical efficiency

Within our research we developed two major concepts for neglecting unwanted wavelet coefficients in order to balance the compression rate against the accuracy of the resulting scattering parameter. The first concept describes a locally fixed grid in the multi-resolution domain for all time-steps, called the static grid. The second approach uses the local energy-density as limiting quantity, which include the corresponding point in the multi-resolution domain, consider the movement by taking the maximum possible velocity into account (light speed) and repeats the re-evaluation with a user defined time-step. We call this compression definition dynamic or adaptive grid, because his structure changes by every reinitiated decision cycles. Both implementations use a so-called mask operator.

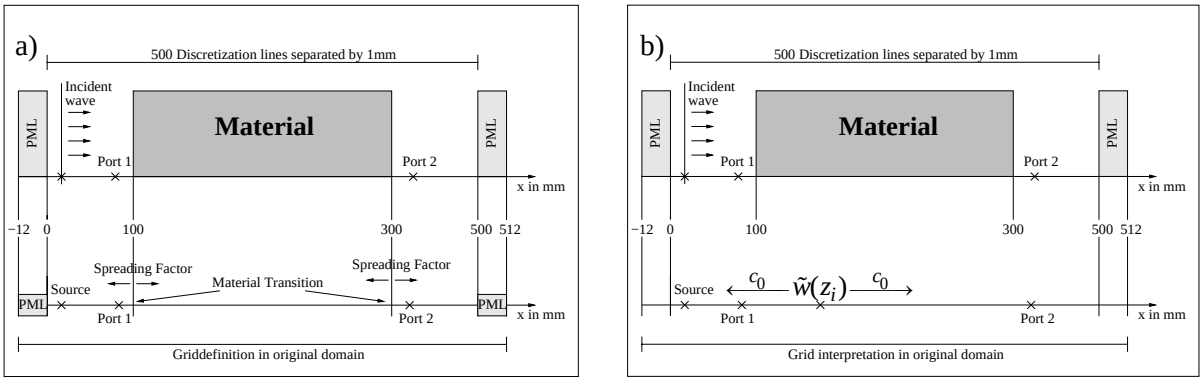

Fig.2 a) depicts the static grid in space. The locally defined points (cross marks) in the original domain are translated into their representative segments V_1 and W_1.

b) depicts the dynamic grid in space. The points (cross marks) are chosen with repeating decision cycle by their assimilated energy density. The possible movement of the energy density is considered by taking light speed into account.

The mask operator $\tilde{S}$ removes unwanted operator coefficients by zero padding, this omits also the corresponding wavelet coefficients of the field-components. The points of interest in the original domain are included into the multi-resolution grid by using the inverse wavelet operator to determine those representative points in the wavelet domain. Using a so called "spreading factor" extends the area around the transition and excitation points $r_{s,i}$ with a defined length n_s and is placed to adjust the desired grid density. All points $\{r_{s,j} \cdots r_{s,j+m}\}$ inside the absorbing boundary and for port scanning are also included statically into the multi-resolution grid. In Fig. 3a we plotted the resulting scattering parameter for conventional and wavelet-transformed FDTD with a dielectric material block (Fig. 2a) using the "haar" filter and a sharing of 55% from the multi-resolution grid. Taking the plot (Fig. 3b) of numerical efficiency into account, we can determine that only the "haar" wavelet simulation with his assigned scattering parameter is working below the numerical costs of the conventional FDTD and the scattering parameters are nearly identical. The calculations of the numerical ratio are weighted with the number of computer cycles for the assigned operation and were determined by equation 2. We experienced no fail estimations using the static grid with one transformation for other material properties, increasing the scale of the operators to two tend into losing agreement for higher frequency. The change of material from lossless to loss property had also no impact on the integral parameters. The static grid strategy got two advantages and one disadvantage. The grid is mainly constructed with experience (a posteriori) and can be changed user-defined before the numerical computation begins. Even for high compression rate the scattering parameter were reliable stable for our chosen examples. The second advantage is not even based on faster computation, but on fewer representative field-components than classical FDTD which yields into less memory consumption. This advantage gives us the opportunity to use our memory resources more efficiently and could tend into simulations which aren't able to compute on available machines yet. One disadvantage behind the static grid definition relays on the challenge finding the right adjustment between wavelet filter and grid density to achieve a better numerical degree of efficiency. For one dimensional wavelet-transformed FDTD schemes the "haar" wavelet seems to be the only choice. Nevertheless we receive some miss coverage on scattering parameters using static grid strategy on high frequency depended material with lossless characteristics, like for the introduced meta-material FDTD scheme modelling [5]. The reason is still under research, but it should be mentioned that the decay of energy inside those structures is very slow and the negligence of field-components alias energy distort the scattering parameter for low frequencies in our used examples. Whereas for dispersive material based on debye-models with the included loss retains good coverage. Custom-built for meta-material simulations we extend the development of dynamic grids (a priori) based on the strategy by Werthen and Wolff [3]. The structure is based on a recurring decision cycle $t_c = n_c \cdot \Delta t$, which determines the local energy density $\tilde{w}(\tilde{r}_j) = \frac{1}{2} \cdot \left(\tilde{\varepsilon} \left| \tilde{E}(\tilde{r}_j) \right|^2 + \tilde{\mu} \left| \tilde{H}(\tilde{r}_j) \right|^2 \right)$ in the multi-resolution grid and include those points $\tilde{r}_j$ in the next cycle which are above a user-defined threshold θ. Since the energy has a direction of movement and a maximum velocity c_0, we also include all points $\tilde{r}_{j\pm n}$ which are in the range $\left|\vec{d}\right| = 2^{-s} n_c \cdot c_0 \cdot \Delta t \wedge n = \frac{|\vec{d}|}{\Delta d}$ around the point $\tilde{r}_j$. In Fig. 4a we plotted the resulting scattering parameter for conventional and wavelet-transformed FDTD for a material block with debye-like dispersion characteristics using the "haar" filter and a threshold of 1e-5 Jm^{-3}. The comparison shows a good match. Taking the plot (Fig. 4b) of numerical efficiency into account, we can determine that every wavelet filter with less than 4 coefficients for the low-pass representation has less numerical effort than conventional FDTD and is independent of the used threshold. The repeating decision cycle was in our case $n_c = 25$ and is an important parameter to reach low computation. The conclusion of the dynamic grid has one advantage and one disadvantage. The downside is high memory consumptions, because the entire transformed scheme needs to be uncompressed and the transformation/inverse wavelet operator is needed to retain a reliable renew process of the grid. The upside shows the independency of wavelet filter and threshold to achieve numerical efficiency. Within the dynamic grid strategy we achieve also better agreement for meta-material, which aren't presented in this paper. The closing question is now how many directions of transformation have the best properties for a 3D spatial wavelet-transformed FDTD scheme. The answer will be given in the next section.

$$Ratio = \frac{wavelet\,transformed\,FDTD\,(Additions + 4 \cdot Multiplications)}{conventional\,FDTD\,(Additions + 4 \cdot Multiplications)} \tag{2}$$

a)

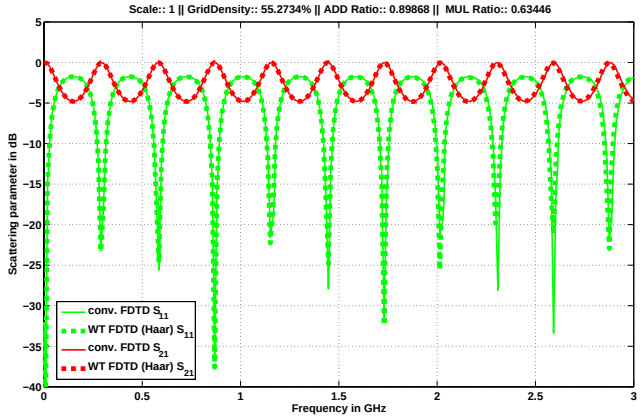

b)

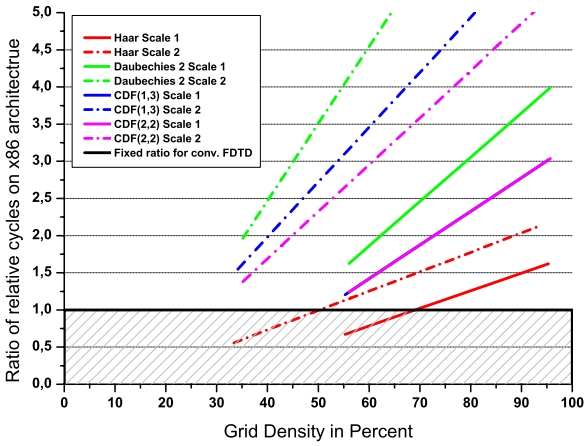

Fig.3. a) Scattering parameter S_{11} and S_{21} for a dielectric block with the permittivity $\varepsilon_r = 10$ within a frequency range from 0 to 3 GHz in comparison of conventional to wavelet-transformed FDTD using static grid strategy

b) Overview of the numerical efficiency with static grid strategy in comparison with conventional and wavelet-transformed FDTD in dependence of the chosen wavelet filter, number of scales and the resulting grid density using a increasing spreading factor.

a)

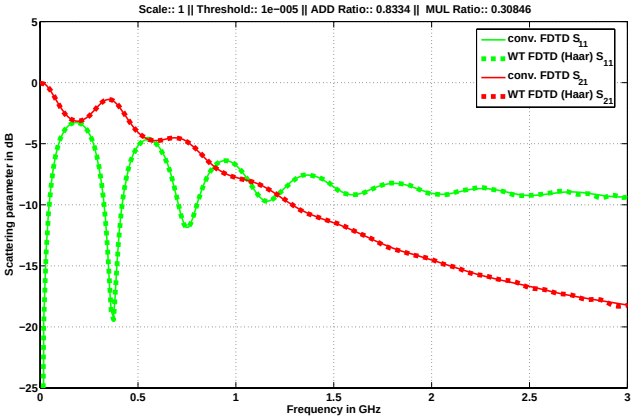

b)

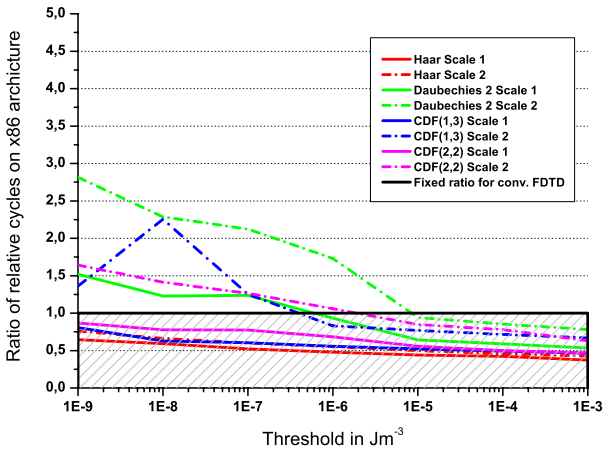

Fig.4. a) Scattering parameter S_{11} and S_{21} for a material block with debye-like dispersion characteristics $\varepsilon_\infty = 4.0 \wedge \Delta\varepsilon = 2 \wedge \tau_0 = 11 \cdot 10^{-11}$s within a frequency range from 0 to 3 GHz in comparison of conventional to wavelet-transformed FDTD using dynamic grid strategy.

b) Overview of the numerical efficiency with dynamic grid strategy in comparison with conventional and wavelet-transformed FDTD in dependence of the chosen wavelet filter, number of scales and using a threshold to neglect unnecessary energy densities.

4. Empirical examination of the microwave structures

The procedure to determine which wavelet filter and which direction of transformation should be included in upcoming FDTD calculation kernels is important with respect to the complexity and time need of pre-processing for the simulation. In previous publication the setup configuration were randomly chosen [3,9,10]. Our publication [6, 7] lighted the needs of appropriate wavelet filter, transformation scheme and assigned deep of scale and will be extended with this paper. The process in this examination is nearly identical mentioned in those publications, were reviewed with extreme precaution and has been extended with many test procedures. A short briefing about the examination process:

1. We simulate several microwave structure with a commercial field solver (EMPIRE) and saved the copy of the electric field-strength for approximately 100 equidistant time steps on the hard disc. The saving starts at the beginning and ends when the energy is nearly absorbed.
2. All copies of the simulation were transformed by using all possible combinations and a transformation deep of zero to one with the wavelet filter (None, Haar, Daubechies 4, Coiflet 6, CDF(1,3), CDF(2,2). With this setup we achieve 216 different constellations.
3. The "non-necessary" wavelet coefficients are set to zero by using static or dynamic grid strategy and the back-transform into the original domain of the compressed field is carried out.
4. The difference using formula (No. 3) between original data E_d and compressed field $\tilde{E}_d$ is determined. The outcome is depicted in figure 5 and 6.
5. The wavelet filter with the lowest error is considered as the most suitable choice for the used multi-resolution grid.
6. We simulate the same microwave structure and settings with swapped coordinate axis and check if the mentioned evaluation process follows the swapped axis.

$$\sigma_{cell} = \frac{\sum_{i=0}^{N_x}\sum_{j=0}^{N_y}\sum_{k=0}^{N_z}\sum_{l=0}^{N_t}\left[\left(\tilde{E}_x - E_x\right)^2 + \left(\tilde{E}_y - E_y\right)^2 + \left(\tilde{E}_z - E_z\right)^2\right]}{N_x \cdot N_y \cdot N_z \cdot N_t} \tag{3}$$

In figure 5 are the top 20 results of a meander line with static grid strategy with different compression levels depicted. The statement of the diagram is the need of only one direction of transformation, mainly the *z*-direction and the most appropriate wavelet filter is nearly unessential, because every possible wavelet filter is in the top 5. The inclusion of one more direction of transformation yields into a jump of mean square error. Figure 6 displays the top 20 results of a patch antenna with dynamic grid strategy using variable thresholds and again can be conclude that one direction of transformation towards the *z* –axis is more than adequate. In both figures the bi-orthogonal Cohen-Daubechies-Feauveau (2,2) is the most suitable one. The investigation about the most appropriate wavelet filter for the calculation of the transformed FDTD scheme is still in process, because the best possible filter changed lightly from structure to structure. The main issue for future FDTD calculation kernels with the spatial wavelet-transformation scheme should be low complexity for the pre-processing and higher efficiency during "leap-frog" calculations. We got for every examined planar microwave structure the same pattern. All examined results shows a uniaxial direction of transformation behavior towards the z-axis, from the ground-plane through the substrate over the metallic sheets into the air. We labeled this pattern of results uniaxial behavior, which stands for low complexity or time need in the build-up of operators inside the pre-processing. We interpreted the uniaxial behavior on the mainly distinctive amplitude of the E_z component above the metallic sheets.

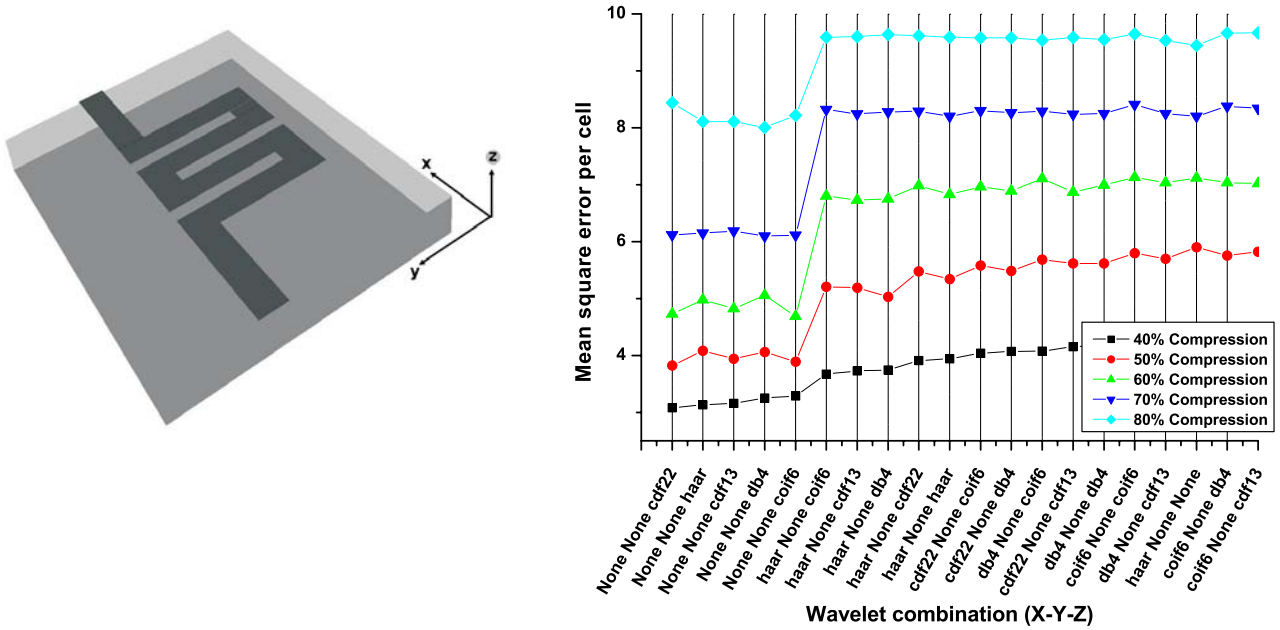

Fig.5. Top20 results (right) of the mean square error using static grid strategy on a meander line (left), the behavior is listed in dependence of chosen wavelet filter, transformation direction and for different compression levels.

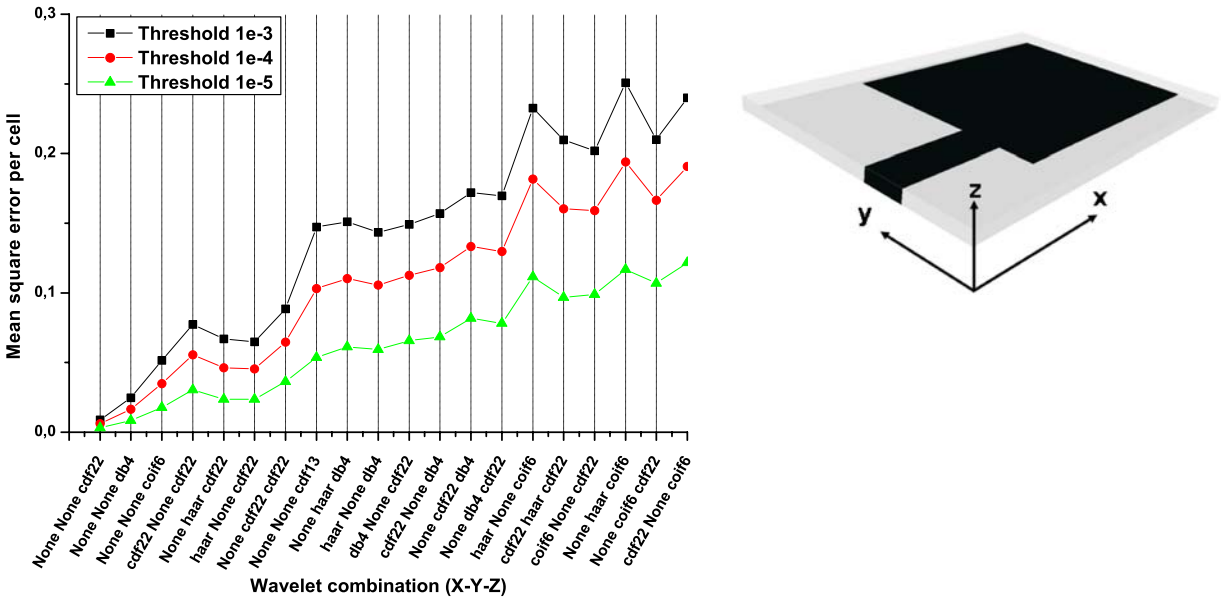

Fig.6. Top20 results (left) of the mean square error using dynamic grid strategy on a patch antenna (right), the behavior is listed in dependence of chosen wavelet filter, transformation direction and for different thresholds.

5. Conclusions

A lot more than the examined scenarios presented in this paper has been investigated by us. All of them support the general idea we got: For an efficient implementation of a spatial wavelet-transformed calculation core and the practice on planar microwave structures there is only a need for an uniaxial transformation scheme towards the normal direction of the metallic sheets or substrate. This concept yields into low complexity or time need in the preparation of operators with spatial multi-resolution capabilities before the computation access the "leap-frog" calculation core. We believe that a well-sophisticated programming concept will need only a few seconds more to compute the pre-processing of uniaxial transformation scheme. Taking the presented numerical efficiency of the one-dimensional spatial wavelet-transformed FDTD scheme into account, we can estimate that our uniaxial transformation scheme achieve less numerical effort than classical FDTD schemes inside the "leap-frog" algorithm and could causes less computation time with proper settings. The right adjustments for the presented neglecting strategies were carried out to achieve higher numerical efficiency for one-dimensional spatial WT-FDTD. Those settings give a good clue how to proceed on upcoming real-world simulation scenarios. Nevertheless both neglecting strategies offer the possibility to score higher numerical capacity. The dynamic grid is faster adjusted for better computational speedup, whereas the static grid definition gives the advantage of less memory consumption. Currently we are developing and implementing a three dimensional spatially wavelet-transformed FDTD calculation kernel with uniaxial transformation scheme to approve our conclusion.

References

[1] M. Krumpholz and L.P.B. Katehi, "New time domain schemes based on multi-resolution analysis", *IEEE Trans. Microwave Theory and Tech.*, Vol. 44, pp. 555-561, 1996.

[2] M. Werthen and I. Wolff, "A novel wavelet based time domain simulation approach", *IEEE Microwave and Guided Wave Letters*, Vol. 6, pp. 438-440, 1996.

[3] M. Werthen and I. Wolff, "A wavelet based time domain moment method for the analysis of three-dimensional electromagnetic fields", *IEEE Trans. Microwave Theory and Tech.*, Vol. 3, pp. 1251-1254, 1998.

[4] W. Bilgic and I. Wolff, "Evaluation of the computational efficiency of a wavelet-transformed FDTD scheme", *European Microwave Conference 2006*.

[5] A. Rennings, S. Otto, A. Lauer, C. Caloz and P. Waldow, "An extended equivalent circuit based FDTD scheme for the efficient simulation of composite right/left handed meta-materials", *Proceedings of the European Microwave Association*, special issue Microwave Meta-Materials, 2006.

[6] W. Bilgic, A. Rennings and P. Waldow, "Evaluation of a multi-resolution grid for the usage in a wavelet-transformed FDTD scheme", *European Microwave Conference 2005*, Vol. 2, pp. 3, Oct. 2005.

[7] W. Bilgic, A. Rennings, P. Waldow and I. Wolff, "Appropriate wavelets with compact support for the compression of FDTD calculated electromagnetic fields", *German Microwave Conference 2005*.

[8] ISO/IEC JTC1/SC29/WG11 N1890, "Information technology – JPEG 2000 Image Coding System.", *www.jpeg.org*

[9] M. Walter and I. Wolff, "An algorithm for realizing Yee's FDTD-method in the wavelet domain", *Microwave Symposium Digest, IEEE MTT-S*, Vol. 3, pp. 1301-1304, 1999.

[10] M. Walter, P. Waldow and I. Wolff, "A wavelet-based FDTD multigrid-method", *Microwave Symposium Digest, IEEE MTT-S*, Vol. 3, pp. 2023-2026, 2001.